Drawability of poly(vinyl alcohol) films prepared by gelation/crystallization from semidilute solutions

Chie Sawatari and Yuko Yamamoto
Faculty of Education, Shizuoka University, Ohya, Shizuoka 422, Japan

and Naoko Yanagida and Masaru Matsuo*
Department of Clothing Science, Faculty of Home Economics, Nara Women's University, Nara 630, Japan
(Received 28 October 1991; revised 6 May 1992)

Poly(vinyl alcohol) (PVA) films prepared by gelation/crystallization from dimethyl sulphoxide/water solutions were drawn in an oven at 125°C under nitrogen. Two PVA samples with degrees of polymerization of 2000 and 4400 were used. The drawability was affected by the composition of the solvent mixture as well as by the quenching temperature. This interesting phenomenon is discussed in terms of the morphology of the gels and dried films, as studied by crystallinity, wide-angle X-ray diffraction, birefringence and small-angle light scattering under *Hv* polarization. Thus, it turned out that crystallinity plays an important role in assuring facile drawability, while the solution concentration and the degree of polymerization have little effect on the drawability. The maximum draw ratio could be achieved only for specimens with the lowest crystallinity. This indicates that the deformation mechanism of PVA gel films is quite different from those of polyethylene and polypropylene gel films.

(Keywords: poly(vinyl alcohol); gelation/crystallization; dimethyl sulphoxide/water; crystallinity; drawability)

INTRODUCTION

Since 1974, the preparation of polymeric fibres and films with high strength and high modulus has been extensively investigated for flexible polymers by gel-state spinning[1], ultra-drawing of dried gel films[2], ultra-drawing of single crystal mats[3], and two-step drawing of single crystal mats[4]. Recently, Matsuo *et al.*, using the method of Smith and Lemstra[2], produced ultra-drawn polyethylene[5] and polypropylene[6] with a Young's modulus at 20°C of 216 and 40.4 GPa, respectively. These values were nearly equal to the crystal lattice moduli of polyethylene[5] and polypropylene[7] as measured by the X-ray diffraction technique.

The results obtained by the method of Smith and Lemstra demonstrate that the effective drawability of high molecular weight polyethylene is dramatically enhanced by using specimens spun or cast from semidilute solutions to form macroscopic gels[8]. For a sufficiently high molecular weight, the maximum achievable draw ratio depends principally on the concentration of the solution from which the gel is made. This phenomenon is attributed to a reduced number of entanglement meshes per molecule in solution cast/spun polymers in comparison with those obtained from the melt.

It should be noted that gels prepared by using low molecular weight polyethylene (LMWPE) ($<4 \times 10^5$) had no ability to form a film[9] and a similar tendency could be observed for low molecular weight polypropylene. In contrast, poly(vinyl alcohol) (PVA) gels with molecular weight $<7 \times 10^4$ have the ability to form a film by evaporating the solvent, and interesting results have been reported[10–13]. For example, Watase and Nishinari[11] reported that the modulus of the gels prepared by freezing/thawing an aqueous atactic PVA solution is higher than that of a gel prepared at temperatures above 0°C and increases by repeating the freezing/thawing cycle. Yamaura *et al.*[13] studied the characteristics of dilute PVA solutions containing dimethyl sulphoxide (Me_2SO) and water (H_2O) and the properties of gels prepared from the solutions. They reported that the turbidity of the solution and the melting point of the resultant gels are dependent upon the ratio of Me_2SO/H_2O. Hyon *et al.*[14] succeeded in producing high modulus PVA fibres by drawing gels prepared by crystallization from semidilute solutions containing 70 vol% Me_2SO, on the basis of a report[15] that solvent mixtures ranging from 50 to 75 vol% Me_2SO do not freeze at −100°C because of hydration. The resultant tensile strength and Young's modulus of the drawn fibre reached 2.8 and 60 GPa, respectively. However, detailed analysis of the deformation mechanism remains an unresolved problem. This paper deals with the deformation mechanism of PVA gel films in terms of morphological aspects as well as the characteristics of PVA molecules in solution.

*To whom correspondence should be addressed

0032-3861/93/050956-11

EXPERIMENTAL

Sample preparation

The samples of PVA powder used had degrees of polymerization ($\bar{P}$) of 2000 and 4400, and a degree of hydrolysis of 98 mol%. The Me_2SO/H_2O compositions chosen as solvent were 100/0, 70/30 and 50/50. The solutions were prepared by heating the well-blended polymer/solvent mixture at 105°C for 40 min. The homogenized solution was poured into an aluminium tray or a Petri dish which was placed into a cold bath set at the desired temperature in the range of −50–100°C for 24 h, thus generating a gel. The gel was vacuum-dried to evaporate the solvent at the chosen temperature. Five combinations of temperatures for gelation/crystallization and evaporation of solvent were used, i.e. methods I–V in *Table 1*. All the resultant dry gel films, which had a thickness of 150 μm, were vacuum-dried for 2 days to remove residual traces of solvent.

The dry gel film was cut into strips of length 40 mm and width 10 mm. The strip was clamped in a manual stretching device in such a way that the length to be drawn was 30 mm. The specimen was placed in an oven at 125°C and was elongated manually to the desired draw ratio under nitrogen flow, since 125°C was the highest temperature to avoid carbonization. After stretching, the stretching device with the sample was cooled slowly to room temperature. Further elongation was carried out under nitrogen at 150–160°C, to a draw ratio, $\lambda > 14$, although the specimens were somewhat yellowed by carbonization.

Sample characterization

The density of the films was measured by pycnometry in a medium of *p*-xylene and carbon tetrachloride. Before the measurements were made, the drawn specimen was cut into fragments and vacuum-dried for 1 day. The crystallinity was calculated by assuming the densities of crystalline and amorphous phases[16] to be 1.345 and 1.269, respectively. The density measurements were carried out several times to check the reproducibility of the values, since the difference in density between crystalline and amorphous phases is not large.

The X-ray measurements were carried out with a 12 kW rotating-anode X-ray generator (Rigaku RAD-rA). Wide angle X-ray diffraction (WAXD) and small angle X-ray scattering (SAXS) patterns were obtained with a flat-film camera using CuKα radiation at 200 mA and 40 kV. The X-ray beam was monochromatized with a curved graphite monochromator. The SAXS intensity distribution in the stretching direction of the specimen was detected with a position-sensitive proportional counter. The measurement was carried out by point focus with a three-pin hole collimator system. The exposure time was 10 days. Detailed measurements have been described elsewhere[9].

Small angle light scattering (SALS) patterns were obtained with a 15 mW He-Ne gas laser as a light source. Diffuse surfaces were avoided by sandwiching the specimen between cover glasses with a silicone immersion oil having a similar refractive index.

Gelation behaviour of the PVA solution was observed in a water bath at a constant temperature. After standing for the desired time, the test tube containing the sample was tilted into the horizontal position. The solution was judged to have gelled when the meniscus could not be seen to deform or the specimen could not flow by itself. In contrast, the gel was annealed in a poly(ethylene glycol) (PEG) bath at a constant temperature to observe gel–sol transition. As in the case of observing gelation, the tube was tilted into the horizontal position after the desired time. When the specimen flowed under its own weight, the gel–sol transition was judged to have occurred. Close observation revealed that the gel tended to be stiffer with storage time. To equalize the storage period of gels, the annealing was done for 100 h.

A cone-plate-type viscometer was employed to investigate viscometric properties of the PVA solutions at certain concentrations in relation to gelation with time. To achieve isothermal conditions in the measurements, the sample cup was thermostatted to ±0.2°C by circulating water around it.

Light transmittance was measured with a Shimadzu UV-240 spectrophotometer at a light wavelength of 570 nm.

Table 1 Preparation methods of PVA films

Method	Temperature (°C)	
	Gelation/crystallization	Evaporation of solvent
I	−50	−50
II	−50	20
III	−20	20
IV	20	20
V	–	100

RESULTS AND DISCUSSION

Figure 1 shows gelation time at the temperatures indicated, as a function of PVA ($\bar{P} = 2000$) concentration

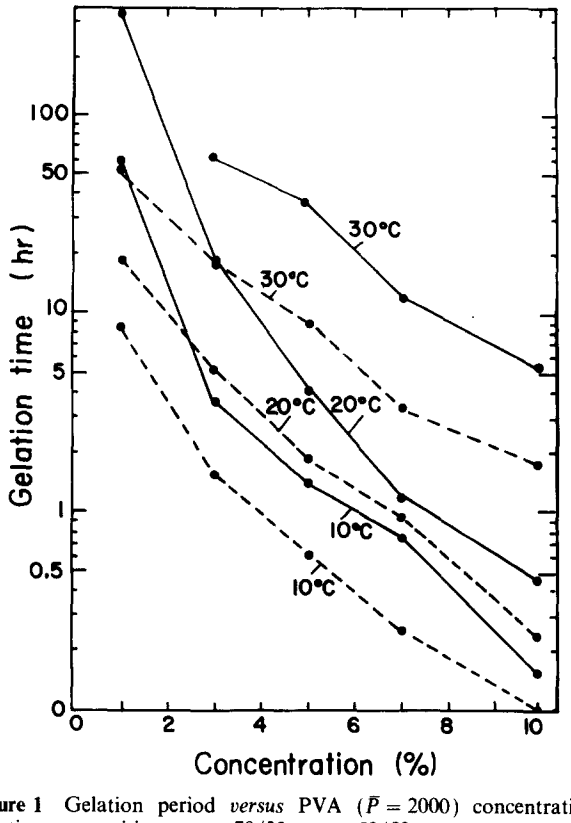

Figure 1 Gelation period *versus* PVA ($\bar{P} = 2000$) concentration. Solution composition: ——, 70/30; – – –, 50/50

in two different mixed solvents (Me_2SO/water), the content of Me_2SO being 70 and 50 vol%. In the following discussion, the solvents will be designated as 100/0, 70/30 and 50/50 compositions. The PVA solution was well stirred in a glass tube in a PEG bath at 110°C and the glass tube was subsequently transferred to a water bath of the desired temperature. The gelation time is taken as the time to form a gel. The gelation time becomes longer with decreasing concentration of solution as well as with increasing temperature of the water bath. The gelation rate of the solution with 50/50 composition is faster than that with 70/30 composition at each fixed temperature and concentration. This indicates that the gelation mechanism is affected by the composition of the mixed solvent.

It was observed that the gel became stiffer with increasing storage time, indicating an increase in cross-linking points due to the promotion of crystallization. The sol–gel and gel–sol transformations show hysteresis. The gelation of PVA solution could not be observed at 85°C but conversely the complete gel–sol transition at 85°C took more than 40 min even for the gel prepared from a 1 w/w% PVA solution with 70/30 composition. This is shown in *Figure 2*. Before the measurements were made, the gel had been stored for 3 days at 20°C. The sol–gel transition time for the gel prepared from solution with 50/50 composition was shorter than that prepared from the solution with 70/30 composition. This behaviour is in good correlation with the time scale of gelation shown in *Figure 1*.

To further substantiate these observations the viscosity was measured as a function of gelation time for the solution at 20°C. *Figure 3* shows the results. The measurements were carried out with a cone-plate-type viscometer for PVA samples with $\bar{P}$ = 2000 and 4400. A solution with 5 w/w% concentration was slowly cooled

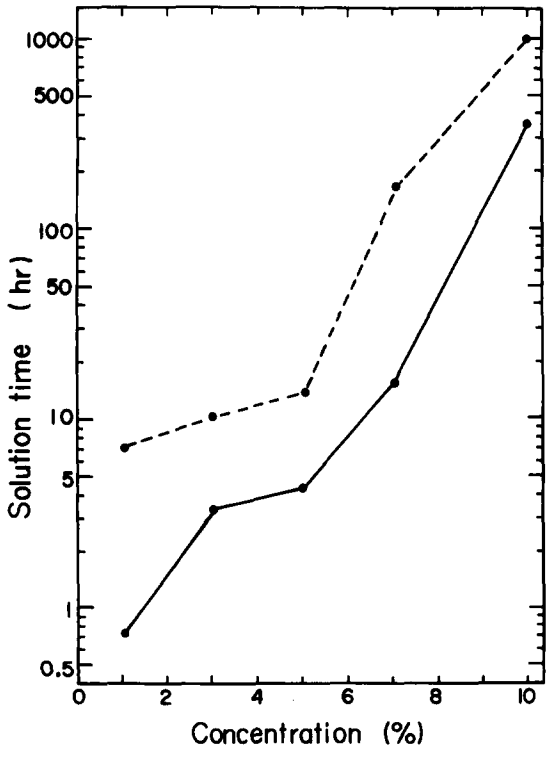

Figure 2 Gel–sol transition at 85°C, observed for PVA ($\bar{P}$ = 2000) gel. Solvent composition (Me_2SO/water): ——, 70/30; – – –, 50/50

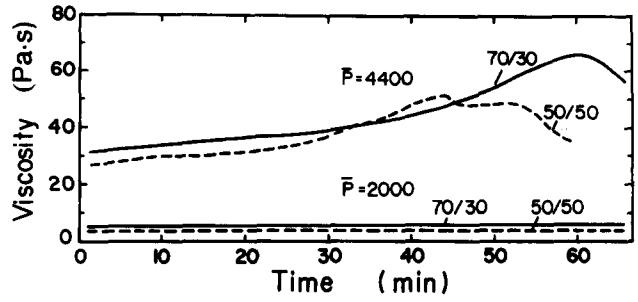

Figure 3 Time dependence of the viscosity of PVA ($\bar{P}$ = 2000 and 4400) solutions with 70/30 and 50/50 compositions at 20°C

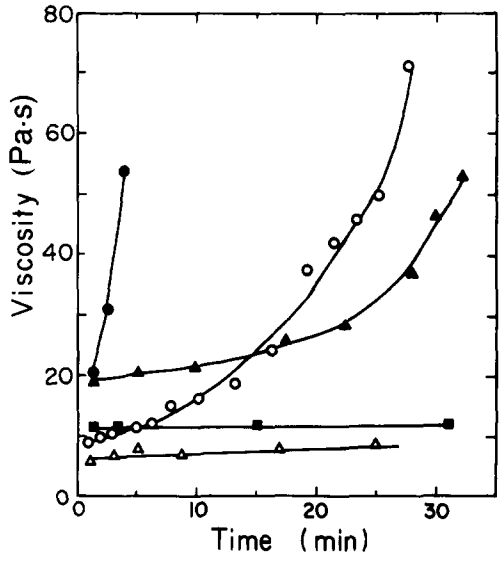

Figure 4 Time dependence of the viscosity of PVA solutions with the 70/30 composition. Solution concentration: open symbols, 5%; solid symbols, 7%. Temperature: ○, ●, 10°C; △, ▲, 20°C; ■, 30°C

to room temperature and then injected into a thermostatted sample cup. The solution was allowed to equilibrate thermally for at least 10 min before starting measurements at a shear rate of 1 s^{-1}. The viscosity of PVA solution with $\bar{P}$ = 2000 remains almost constant, with values of 5 and 3 Pa s for 70/30 and 50/50 solvent compositions, respectively. On the other hand, the viscosity of the solution with $\bar{P}$ = 4400 increases with time for both solutions because of promotion of gelation. For the solution with 50/50 composition, the collapse of gel occurred when the viscosity reached 50 Pa s. Therefore, the viscosity decreased with time. A similar tendency was observed for the solution with 70/30 composition but the period to the yield point is longer than that for the 50/50 composition.

Even for PVA solutions with $\bar{P}$ = 2000, whose viscosity is independent of time under the above conditions, the gelation mechanism depends on the concentration of the solution and on the temperature of the measurements. *Figure 4* shows an example for solutions with 70/30 composition. The increase in viscosity with time becomes more pronounced with increasing concentration of the solution and with decreasing temperature.

The dependence of the gelation mechanism on the degree of polymerization was also confirmed by light transmittance measurements, which are not shown. The absorption of light was more pronounced as the storage time of gels increased, because of the progression of the

gelation. Interestingly, the light transmittance was much more sensitive to the composition than the degree of polymerization, which contrasts with the time-dependence of viscosity shown in *Figure 3*. The gels prepared from solutions with 70/30 composition were much more transparent than those from the solution with 50/50 composition. Two causes can be considered for this phenomenon: (1) the difference of spinodal decomposition rate[17]; and (2) the difference of gelation rate as shown in *Figures 1* and *2*. The former will be discussed elsewhere[18].

The gelation mechanism of PVA ($\bar{P} = 2000$) was further investigated by X-ray diffraction as a function of storage time. *Figure 5* shows the WAXD patterns of gels prepared from the solution with 70/30 composition by method IV. The WAXD pattern exhibits a very weak diffraction ring from the (1 0 1) and (1 0 $\bar{1}$) planes, indicating crystallization at a storage time less than 8 h. The patterns (*Figures 5a–d*) indicate the promotion of crystallization with increasing storage time. X-ray patterns were also obtained for the gels prepared from the solution with 50/50 composition. Similar patterns were observed but the diffraction rings appeared at an earlier stage in comparison with the solution with 70/30 composition.

In order to ascertain the relationship between gelation mechanism and drawability of the resultant dried films, the maximum draw ratio was determined for PVA films prepared under various conditions, as listed in *Table 2*. In *Table 2*, the maximum draw ratio of the gel film prepared by method I is listed as a function of the composition of the mixed solvent consisting of Me_2SO and water. It is seen that the 70/30 composition provided the maximum value of the draw ratio, 12.5, at any given solution concentration. Furthermore the drawability was found to be more sensitive to the Me_2SO/H_2O

Table 2 Maximum draw ratio (λ_{max}) of the dried gel films prepared from solutions with different Me_2SO/water compositions and concentrations

		Concentration (g/100 ml)			
Me_2SO/water	Method	5[a]	10[a]	2[b]	5[b]
100/0	I	9	6	9	8
70/30	I	12.5	12.5	12.5	12.5
	II	12.5	12.5	12.5	12.5
	III	12	11	12	12
	IV	10	10	9	9
	V	7	6	8	6
50/50	I	11	11	11	11

[a] $\bar{P} = 2000$
[b] $\bar{P} = 4400$

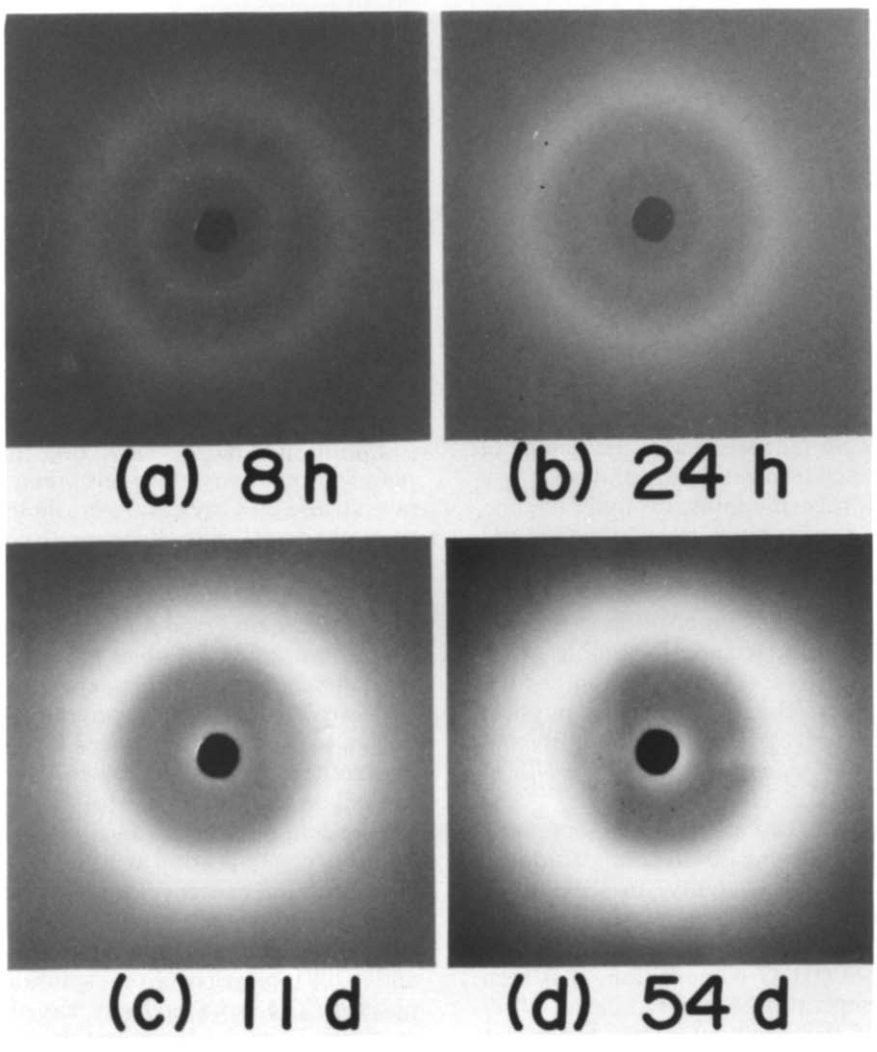

Figure 5 WAXD patterns as a function of storage time: (a) 8 h; (b) 24 h; (c) 11 days; (d) 54 days. The gels were prepared by method IV

Table 3 Characteristics of drawn films prepared by method I

$\bar{P}$	Concentration (g/100 ml)	Composition (Me_2SO/H_2O)	Storage modulus (GPa)	λ	Crystallinity (%)	Birefringence ($\times 10^3$)
4400	5	50/50	25.5	11	43	43.5
		70/30	30.0	12.5	44	44.5
		100/0	19.4	8	34	40.4
	2	50/50	29.5	12	42	45.7
		70/30	31.4	12.5	45	48.1
		100/0	27.2	9	39	43.6
2000	10	50/50	26.6	11	41	43.6
		70/30	28.5	12.5	44	45.4
		100/0	22.0	6	29	20.5
	5	50/50	25.0	11	26	45.1
		70/30	27.1	12.5	27	46.2
		100/0	22.3	9	21	42.6

Table 4 Crystallinity (%) of films prepared from solutions with different Me_2SO/water compositions and concentrations

Me_2SO/water	Method	Concentration (g/100 ml)			
		5[a]	10[a]	2[b]	5[b]
100/0	I	17	29	27	27
70/30	I	10	20	23	23
	II	13	26	25	26
	III	18	32	32	34
	IV	21	34	33	34
	V	26	22	23	47
0/100	I	12	22	24	25

[a] $\bar{P} = 2000$
[b] $\bar{P} = 4400$

composition than the concentration of solution. *Table 2* also lists the maximum draw ratio of each film prepared from solutions with various concentrations by methods I–V, in which the content of the mixed solvent was fixed to be the 70/30 composition. The draw ratios shown are the highest values corresponding to a gelation temperature of −50°C. The maximum draw ratios of films prepared by methods I and II were independent of the degree of polymerization and the concentration of solution.

Table 3 lists the storage modulus, crystallinity and birefringence of films with maximum draw ratio prepared by method I. The measurements were made at 20°C. The degree of polymerization of PVA, the concentration of solution to form a gel, and the composition of solvent were adopted as parameters. It should be noted that among these three parameters, the composition has the most significant effect on the value of the physical properties. That is, the storage modulus, crystallinity and birefringence showed the highest values at the 70/30 composition.

Here a question can be raised as to why the specimen prepared from solutions with the 70/30 composition by method I has the highest drawability. In seeking an answer to this question, the crystallinity was measured for undrawn films. *Table 4* lists the crystallinity of films as a function of the Me_2SO/H_2O composition. It is seen that the quenching temperature has a significant effect on the crystallinity of the resultant films, except for method V. In particular, the crystallinity of the samples prepared from solutions with 70/30 composition by method I has a lowest value at the specified degree of polymerization and concentration. Since the samples prepared from solutions with 70/30 composition show the highest drawability, this can be rationalized by assuming that the solvent with 70/30 composition is a good solvent for PVA and the size or spatial extension of PVA molecules in solution becomes greatest at a fixed concentration. Actually, the specific viscosity, η_{sp}, at the 70/30 composition was higher than that at the 50/50 composition at 100°C[18]. Therefore, the solution is thought to consist of interpenetrating random coils which form a large number of intermolecular coupling entanglements. In contrast, the number of intramolecular coupling entanglements is thought to be the lowest. Thus, it may be expected that the coupling entanglements are characteristic of the solution that hampers the formation of crystallites as cross-linking points on quenching. This tendency becomes more marked as the gelation (quenching) temperature becomes lower. As discussed before, after the solution was quenched to −50°C and subsequently the resultant gel was vacuum-dried at −50°C (method I), the crystallinity of the resultant film took the lowest value.

Figures 6a and *b* show SALS patterns under *Hv* polarization observed for gels prepared by crystallization at −20 and 20°C, respectively; these methods are similar to methods III and IV, respectively. The photographs were taken after the gels ($\bar{P} = 2000$) had been stored for 2 days at 20°C without evaporating solvent. The same profiles were observed for gels with $\bar{P} = 4400$. Similarly, no pattern could be observed for the gel prepared by crystallization at −20°C in spite of the appearance of a very weak X-ray diffraction ring from the crystallites. Such a tendency was observed for the gel films prepared by method I. This indicates random orientation of crystallites that are much smaller than the wavelength of the incident laser beam. In contrast, the gel prepared by gelation/crystallization at 20°C shows an X-type pattern, indicating the existence of anisotropic rods, the optical axes being oriented parallel or perpendicular to the rod axis[16]. The same profile was observed for gels ($\bar{P} = 2000$ and 4400) prepared from solution with 50/50 composition. The same tendency was observed for the dried gel films. Thus, it is apparent that gel structure depends on the gelation temperature and the appearance of

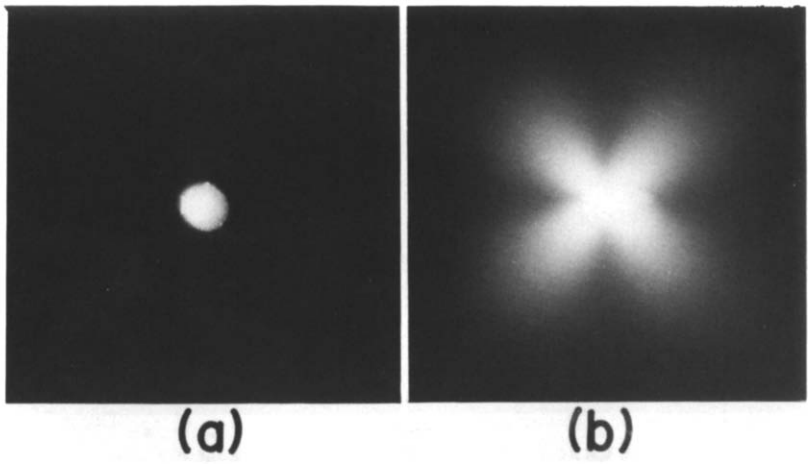

Figure 6 SALS patterns (a) and (b) under *Hv* polarization condition observed for gels prepared by crystallization at −20 and 20°C, respectively

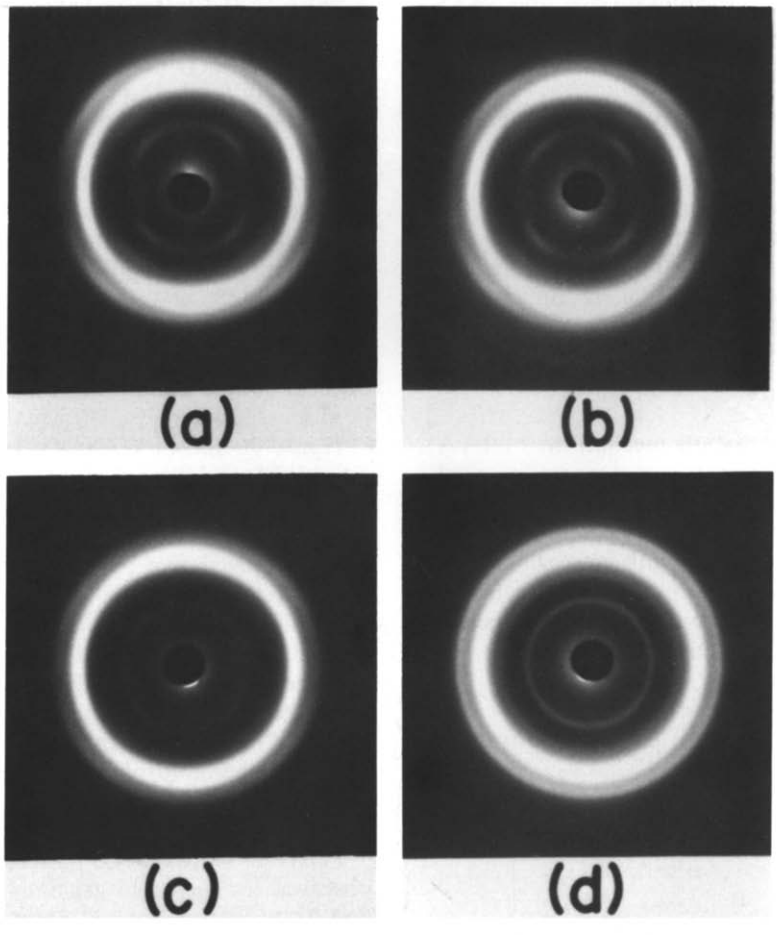

Figure 7 WAXD patterns (end view) of dried gel films: (a) method I; (b) method II; (c) method IV; (d) method V

rod-like textures detected by SALS hampers the facile drawability of the resultant dry gel film. Here it may be noted that the crystallinities were 13% and 18% for the specimens prepared by method II and III, respectively (*Table 4*), and the formation of superstructure is related to the small difference of crystallinity.

Incidentally, the X-type patterns from gels could not be observed by the usual method. That is, the scattered beam from the gels could not be transmitted through the analyser because of very weak scattered intensity. The *Hv* pattern was obtained from the gel film surface using the scattered beam reflected from the analyser, which plays the role of a reflecting mirror. Instead of using a flat camera, the *Hv* light scattering patterns were observed as photographs taken through the analyser with a suitable camera.

To investigate the structure of gels in relation to the gelation temperature, WAXD patterns (end view) of dried gel films prepared by methods I, II, IV and V were taken, as shown in *Figure 7*. The WAXD patterns of the gel films obtained by methods I, II and IV, respectively (*Figures 7a–c*), suggest a slight uniplanar orientation of the (1 0 1) plane parallel to the film surface, probably due to the small planar tension during gelation. In

contrast, the pattern of the film prepared by method V (*Figure 7d*) exhibits diffraction rings, indicating a random orientation of crystallites. To obtain more detailed information, SAXS measurements were made.

Unfortunately, three kinds of SAXS patterns (end view) of the films prepared by methods II, IV and V show no scattering from crystal lamellae and only void scattering in the horizontal direction can be observed. These patterns are not shown. The WAXD and SAXS patterns together indicate that the uniplanar orientation of the (1 0 1) plane can be explained in terms of the slip of the (1 0 1) plane associated with its orientation parallel to the planar stress. The (1 0 1) plane has the highest electron density within the crystal unit cell and the uniplanar orientation must be attributed to lowering of the dislocation energy of the plane. This is quite different from the process of formation of gel structures of polyethylene[20] and polypropylene[6]. In these latter cases, the WAXD patterns indicate a preferential orientation of the *c*-axes perpendicular to the film surface, and SAXS patterns indicate the existence of crystal lamellae highly oriented with their large flat faces parallel to the film surface.

From the X-ray diffraction experiments discussed above, it may be concluded that the PVA crystallites are too small to be detected by SAXS measurements and the crystal fibre axis (the *b*-axis) is oriented parallel to the film surface. However, the experimental results do not give any information as to whether the crystallites are of the folded or fibrous type. Thus, it is difficult to understand the deformation mechanism of PVA gel films in comparison with the experimental results obtained already for polyethylene[20,21] and polypropylene[6] gel films.

To understand the deformation mechanism of PVA gel films, their morphological properties were investigated by using specimens ($\bar{P} = 4400$) prepared by methods I–V from 5 w/w% solutions with 70/30 composition. *Figure 8* shows the change in birefringence with increasing draw ratio λ. The measurements were made on specimens prepared by method I. The birefringence with respect to the stretching direction was estimated by the method proposed by Stein for biaxially oriented films[22]. The birefringence shows a considerable increase up to $\lambda = 4$ but it increases slowly beyond $\lambda = 4$. The maximum value

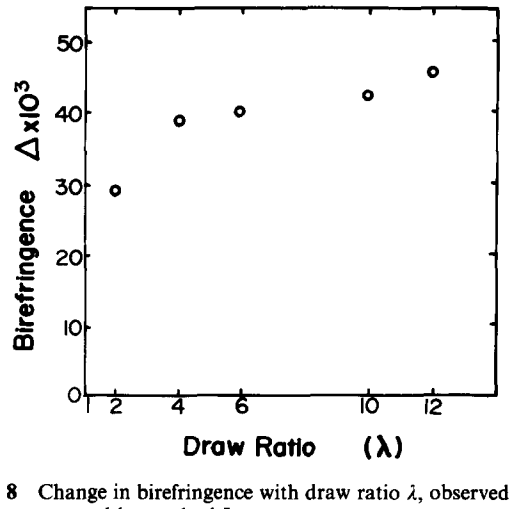

Figure 8 Change in birefringence with draw ratio λ, observed for the specimen prepared by method I

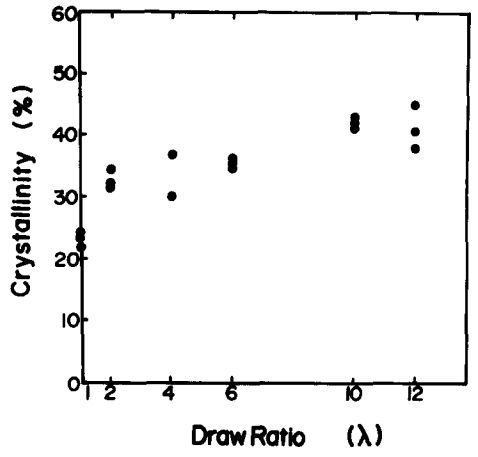

Figure 9 Change in crystallinity with draw ratio λ, observed for specimen prepared by method I

is close to the intrinsic value (48.4×10^{-3}) which can be calculated by assuming the atomic arrangements within the crystal[23] and the values of the bond polarizabilities[24], and by neglecting the uncertain effects of the internal field within the crystal and of secondary bonds upon the principal polarizabilities. The birefringence at $\lambda = 12$ indicates an almost perfect orientation of PVA molecules with respect to the stretching direction.

Figure 9 shows crystallinity as a function of λ. The crystallinity shows a gradual increase with λ and it attains a value of 44% at $\lambda = 12$. This value is much lower than the values reported for ultradrawn polyethylene and polypropylene[8]. This hampers the drastic improvement of the Young's modulus of the drawn PVA films, as will be discussed later.

Figure 10 shows WAXD patterns of PVA films with $\lambda = 12$. The gel films were prepared under the conditions indicated. The patterns exhibit a high degree of orientation of the *b*-axis with respect to the stretching direction, as shown by the small angular spread of the strong reflections from each crystal plane. This high orientation was independent of the preparation methods I, II and III. The orientation is not significant for the specimen prepared by method V, although it is not shown in this paper. Because of low crystallinity in *Figure 9*, the birefringence values of the specimens with $\lambda > 6$ in *Figure 8* indicate that amorphous chain segments are also highly oriented with respect to the stretching direction, in addition to a high degree of orientation of the *b*-axis.

Figure 11 shows SALS patterns under *Hv* polarization observed for the dried gel films prepared by methods I and II as a function of draw ratio. Incidentally, the specimens with $\lambda > 14$ were prepared by second elongation under nitrogen at 150–160°C using films drawn up to $\lambda = 12$ at 125°C. The specimens were somewhat yellowed by carbonization. The scatterings from undrawn films prepared by methods I and II display indistinct circular patterns in which the intensity decreased continuously with increasing scattering angle but does not vary with the azimuthal angle. This is typical of the scattering from a system composed of a random array of crystallites that are small compared with the wavelength of incident beam. For both films, elongation up to $\lambda = 2$ causes development of a clear X-type pattern whose lobes are extended in the horizontal direction, indicating the preferential orientation of rods in the stretching direction[19]. In contrast, elongation beyond

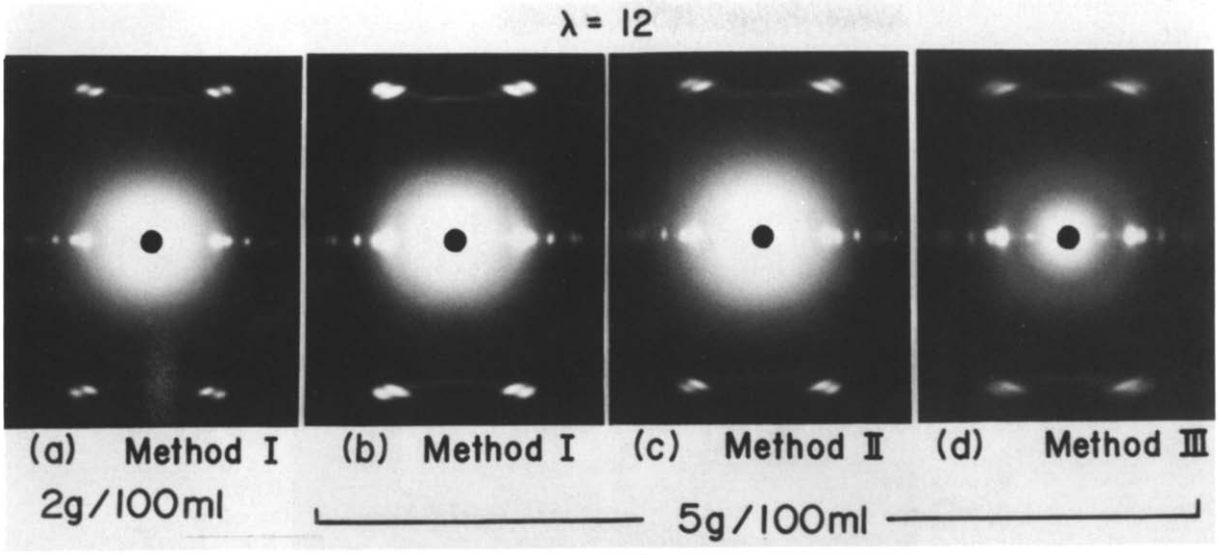

Figure 10 WAXD patterns (through view) of drawn films: (a) method I (2 g/100 ml); (b) method I (5 g/100 ml); (c) method II; (d) method III

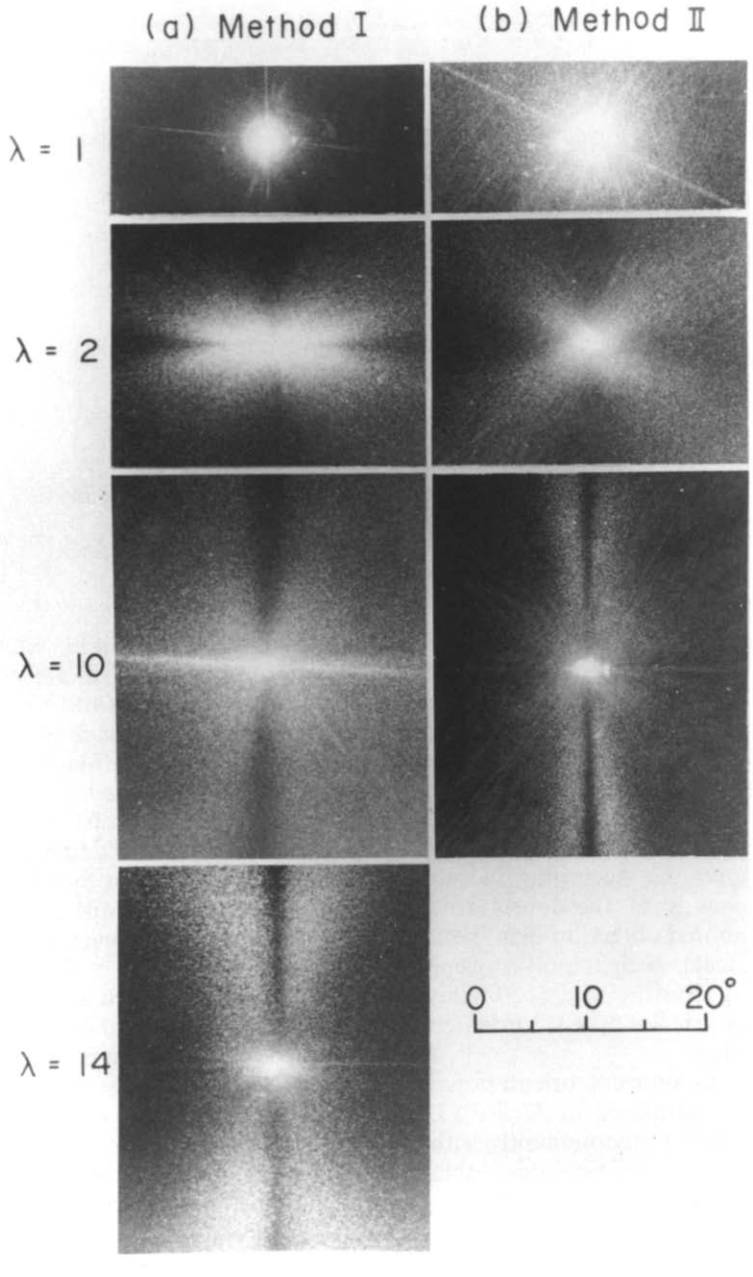

Figure 11 *Hv* light scattering patterns observed for the dried films prepared by (a) method I and (b) method II, at various draw ratios

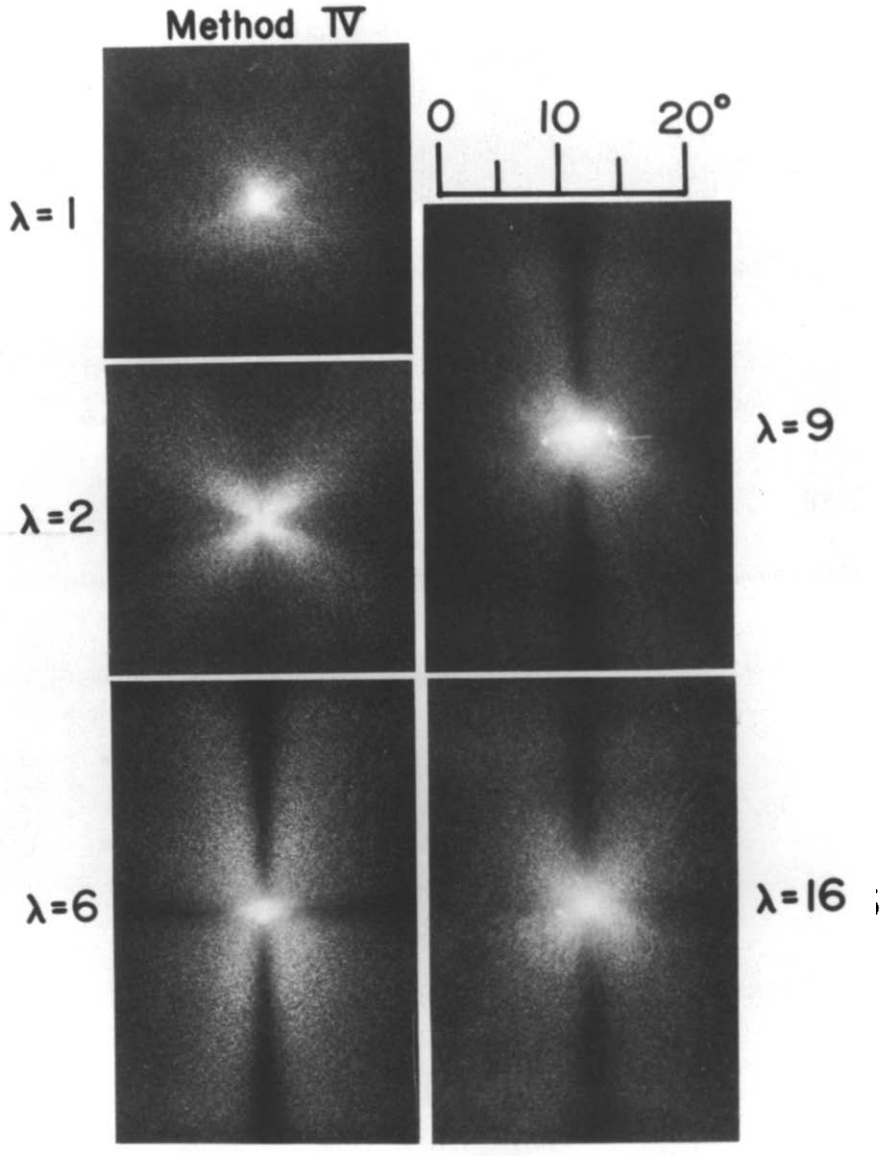

Figure 12 *Hv* light scattering patterns observed for the dried films prepared by method IV, at various draw ratios

$\lambda = 10$ gives an X-type pattern whose lobes are extended in the meridional direction. Considering the theory of SALS under *Hv* polarization, such sharp lobes must be interpreted as a contribution of scattering from rods with extremely high orientation perpendicular to the stretching direction. Such a drastic change of orientation behaviour of rods with $\lambda < 10$, however, is quite unexpected. A similar profile was observed for the gel film prepared by method IV, as shown in *Figure 12*. According to our earlier work[25], a drastic change of the lobes from the horizontal to the meridional direction has been observed for ultra-high molecular weight polyethylene (UHMWPE) gel films during drawing at $\lambda > 20$. This phenomenon was confirmed to be due to oriented crystallization during elongation.

In order to explain such an unusual orientational behaviour of rods, a model is proposed in *Figure 13*. *Figure 13a* represents rods oriented predominantly with respect to the stretching direction. The crystallites within a rod are connected to each other and the crystal axis, corresponding to the optical axis, is oriented predominantly parallel to the stretching direction. *Figure 13b* is proposed to explain the profile of the scattering pattern whose lobes are extended in the meridional direction. As shown in *Figure 13b*, a scattering unit corresponds to a new rod-like structure that is formed by a lateral coalescence of rods during elongation. Thus, the scattering unit within the film at $\lambda > 6$ is different from that at $\lambda = 2$ (see *Figure 11*) and this model is consistent with the drastic change of the profile of the patterns without considering any unusual orientation of rods. To fully confirm the above concept, the existence of crystal lamellae within the drawn film must be confirmed by SAXS measurements. *Figure 14* shows a pattern observed for a film with $\lambda = 6$, prepared by method II. The pattern exhibits the first order scattering maximum in the meridional direction, corresponding to a long period of 12.3 nm. A similar profile was observed for a specimen with $\lambda = 10$. Unfortunately, the scattering maximum was too indistinct to show the pattern here. This is probably due to the fact that the difference of electron density between crystal and amorphous phases is too small to give a distinct scattering maximum of SAXS intensity distribution in the meridional direction. Another method must be considered to confirm the existence of crystal lamellae.

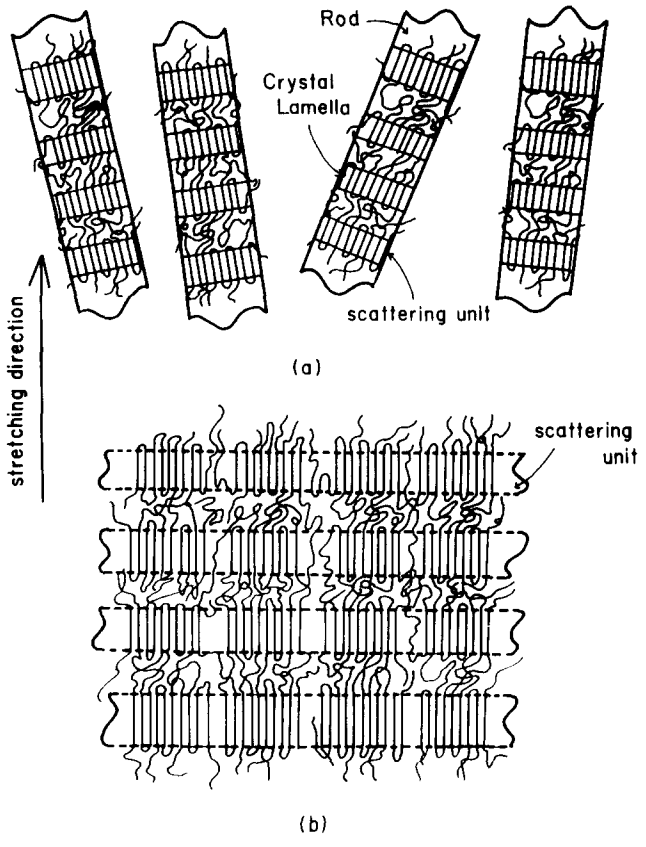

Figure 13 Model proposed to explain change in *Hv* light scattering patterns in *Figures 11* and *12*

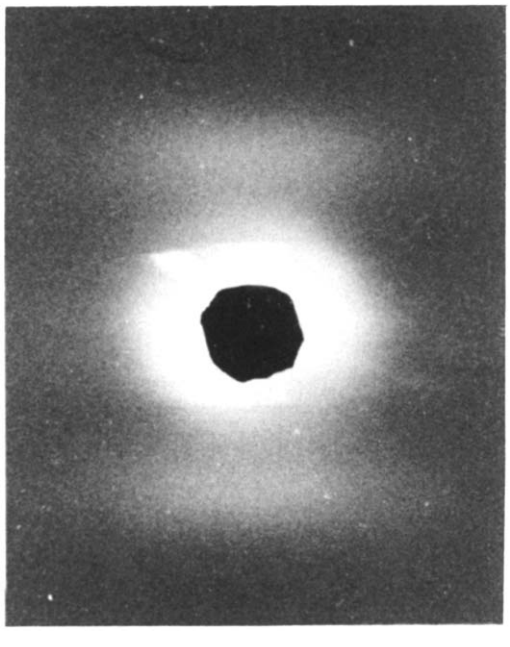

Figure 14 SAXS pattern obtained for the dried gel films with $\lambda = 6$, prepared by method II

Figure 15 shows the nominal stress–elongation curves at 20°C for the dried gel films prepared by methods I and IV. In determining the stress corresponding to each elongation, the value of the tensile force was divided by the cross-sectional area of the original specimen. The stress increases drastically up to the yield point. The yield point of the film prepared by method IV is higher than

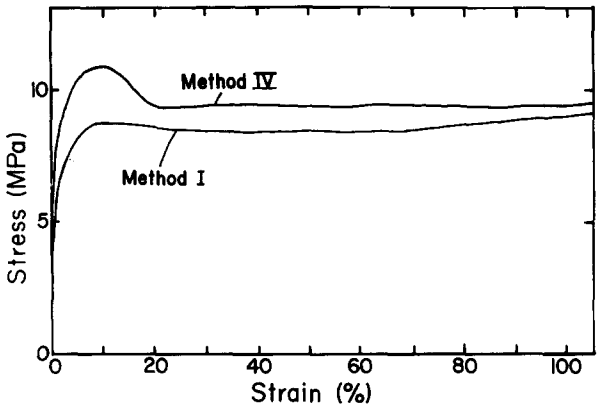

Figure 15 Nominal stress–elongation curves for the dried gel films prepared by methods I and IV

that preferred by method I. This is probably due to higher crystallinity of the former undrawn film (34%) in comparison with the latter (23%). Beyond the yield point, the stress decreases and tends to level off. If the tensile force is divided by the cross-sectional area of the specimen at each elongation, the stress, of course, increases with draw ratio.

It was visually observed that the deformation process is almost uniform even in the initial stages of elongation, although the decrease in transverse specimen dimension with increasing length occurs mainly in the film thickness and slightly less in the film width. Such a deformation mechanism is quite different from that of polyethylene and polypropylene gel films associated with necking. For polyethylene and polypropylene films, the elongation regions were enlarged at the expense of the undrawn zone and the drawing process was non-uniform, indicating significant crystal transformation from a folded to a fibrous type[20].

In summary, the PVA chains were fully aligned by elongation of dried gel films that were produced by crystallization from solution with 70/30 composition. Unfortunately, the Young's modulus was much lower than that of ultra-drawn polyethylene, in spite of the fact that the crystal lattice modulus of PVA (240 GPa)[26] is higher than that of polyethylene (222–229 GPa)[5]. This is probably due to the low degree of crystallinity of the PVA sample, which was less than 50%, as discussed in *Figure 9*. This phenomenon was demonstrated by using UHMWPE–LMWPE blended gel films; the Young's modulus of ultra-drawn polyethylene gel films ($\lambda = 200$) with 94% crystallinity was 130 GPa, while that of the blended film with the same value of λ and a crystallinity of 82% was 81 GPa, in spite of having almost the same birefringence value[27]. Thus, it may be concluded that crystallinity plays an important role in the production of high modulus polymeric materials, in addition to molecular orientation. To produce an ideal sample of PVA whose Young's modulus is close to the crystal lattice modulus, it may be concluded that a drastic increase in crystallinity must be realized by elongation.

CONCLUSION

The drawability of PVA has been studied as a function of degree of polymerization, composition of mixed solvent, concentration of solution and the temperature of gelation/crystallization. Through a series of experiments,

it was found that the maximum draw ratio could be realized when the gel was prepared from a solution with 70/30 composition by quenching at −50°C. The crystallinity was lowest under these conditions and no superstructure such as a rod-like texture could be observed by SALS under *Hv* polarization. Thus it turned out that the deformation mechanism of PVA is rather similar to that of amorphous poly(ethylene terephthalate) films, but it is quite different from ultra-drawing of polyethylene and polypropylene, which is associated with a significant crystal transformation from a folded to a fibrous structure. The maximum value of the storage (Young's) modulus was about 31.4 GPa in spite of an almost perfect alignment of the molecular chains. This value is much lower than the crystal lattice modulus and this is attributed to low crystallinity $< 50\%$ of the drawn films.

ACKNOWLEDGEMENTS

We are indebted to Professor M. Watase of the Faculty of Liberal Arts, Shizuoka University for his valuable comments and suggestions. Thanks are also due to Professor R. St J. Manley, Department of Chemistry, Pulp and Paper Research Centre, McGill University, for his kind help with linguistic revision of the manuscript.

REFERENCES

1 Smith, P. and Lemstra, P. J. *J. Mater. Sci.* 1980, **15**, 505
2 Smith, P., Lemstra, P. J., Pipper, J. P. L. and Kiel, A. M. *Colloid Polym. Sci.* 1980, **258**, 1070
3 Furuhata, K., Yokokawa, T. and Miyasaka, K. *J. Polym. Sci., Polym. Phys. Edn* 1984, **22**, 133
4 Kanamoto, T., Tsuruta, A., Tanaka, K. and Porter, R. S. *Polym. J.* 1983, **15**, 327
5 Matsuo, M. and Sawatari, C. *Macromolecules* 1986, **19**, 2036
6 Matsuo, M., Sawatari, C. and Nakano, T. *Polym. J.* 1986, **18**, 759
7 Sawatari, C. and Matsuo, M. *Macromolecules* 1986, **19**, 2653
8 Smith, P., Lemstra, P. J. and Booij, H. C. *J. Polym. Sci., Polym. Phys. Edn* 1981, **19**, 877
9 Sawatari, C., Okumura, T. and Matsuo, M. *Polym. J.* 1986, **18**, 741
10 Watase, M., Nishinari, K. and Nambu, M. *Polym. Commun.* 1987, **24**, 52
11 Watase, M. and Nishinari, K. *Macromol. Chem.* 1988, **189**, 871
12 Yamaura, K., Karasawa, T. and Matsuzawa, S. *J. Appl. Polym. Sci.* 1987, **34**, 2347
13 Yamaura, K., Karasawa, T. and Matsuzawa, S. *J. Appl. Polym. Sci.* 1989, **37**, 2709
14 Hyon, S. H., Cha, W. I. and Ikada, Y. *Reports of Poval Committee* 1989, **37**, 2709
15 Farrant, J. *Nature* 1965, **205**, 1284
16 Sakurada, I., Nukushina, K. and Sone, Y. *Kobunshi Kagaku* 1955, **12**, 506
17 Komatsu, M., Itoh, M., Tanigami, T. and Matsuzawa, S. *J. Polym. Sci.* 1986, **24**, 303
18 Matsuo, M., Kawase, M., Sugiura, Y. and Takematsu, S. in preparation
19 Rhodes, M. B. and Stein, R. S. *J. Polym. Sci., A-2* 1969, **7**, 1538
20 Matsuo, M. and Manley, R. St J. *Macromolecules* 1982, **15**, 985
21 Matsuo, M., Sawatari, C., Iida, M. and Yoneda, M. *Polym. J.* 1985, **17**, 1197
22 Stein, R. S. *J. Polym. Sci.* 1957, **24**, 383
23 Nitta, I., Taguchi, I. and Chatani, Y. *Ann. Rept. Inst. Fiber Sci. Osaka Univ.* 1957, **10**, 1
24 Clement, C. and Botherel, P. *C. R. Acad. Sci. (Paris)* 1964, **258**, 4757
25 Matsuo, M., Inoue, Y. and Abumiya, N. *Seni- Gakkaishi* 1984, **40**, 275
26 Sakurada, I., Ito, T. and Nakamae, T. *J. Polym. Sci. C* 1966, **15**, 75
27 Sawatari, C. and Matsuo, M. *Polymer* 1989, **30**, 1603